Letter

Axion-photon multimessenger astronomy with giant flares

Javier De Miguel* and Chiko Otani

The Institute of Physical and Chemical Research (RIKEN), Center for Advanced Photonics, 519-1399 Aramaki-Aoba, Aoba-ku, Sendai, Miyagi 980-0845, Japan

(Received 13 January 2022; accepted 29 June 2022; published 25 August 2022)

We treat prospects for multimessenger astronomy with giant flares (GFs), a rare transient event featured by magnetars that can be as luminous as a hundred of the brightest supernovae ever observed. The beamed photons could correlate with an axion counterpart via resonant conversion in the magnetosphere. In a realistic parameter space, we find that the sensitivity limit to Galactic GFs for currently viable experiments is $g_{\phi\gamma} \gtrsim$ several $\times 10^{-13}$ GeV^{-1} and $g_{\phi e} \gtrsim$ few $\times 10^{-12}$. We rule out the compatibility of axion flares with the recent XENON1T excess only due to the time persistence of the signal.

DOI: 10.1103/PhysRevD.106.L041302

I. BACKGROUND

The quantum chromodynamics (QCD) axion [1,2] is a hypothetical pseudoscalar boson that arises from the dynamic solution to the charge and parity (CP) problem in the strong interaction [3]. The axion mass, m_ϕ, and coupling constant, g, are unknown in spite of the remarkable effort realized to find axions in the parameter space at which that can simultaneously solve the CP problem and the dark matter (DM) enigma [4–7]. Relevant interactions of axionlike particles to Standard Model (SM) particles for this work are

$$\mathcal{L}^{\rm int} = -\frac{1}{4} g_{\phi\gamma} F_{\mu\nu} \tilde{F}^{\mu\nu} \phi + i g_{\phi e} \bar{\psi} \gamma^5 \psi \phi, \tag{1}$$

where the first term on the right-hand side represents the effective axion-photon Lagrangian density and the second term repesents the axion-electron coupling; ϕ being the axion field, $F^{\mu\nu}$ the photon field, ψ the electron field, and γ_5 the usual matrix.

II. AXION-PHOTON MIXING IN ASTROPHYSICAL ENVIRONMENTS

A. General mixing relations

Aided by axion electrodynamics [8] for the linearization of the equations of motion from Eq. (1), a set of Schrödinger-like dispersion relations emerges that can be solved analytically in idealized astrophysical boundaries [9]

$$\left[\omega + \begin{pmatrix} \Delta_\perp + \Delta_{Q_\parallel} & \Delta_R & \Delta_{M_x} \\ \Delta_R & \Delta_p + \Delta_\parallel + \Delta_{Q_\perp} & \Delta_{M_y} \\ \Delta_{M_x} & \Delta_{M_y} & \Delta_\phi \end{pmatrix} - i\partial_z \right] \begin{pmatrix} E_\perp \\ E_\parallel \\ \phi \end{pmatrix} = 0. \tag{2}$$

The interaction term $\mathcal{L}^{\phi\gamma} = g_{\phi\gamma} E \cdot B$ is obtained from Eq. (1); E being the photon and B the external magnetic field, establishing a preferential polarization. Now, obviating the Faraday rotation term, Δ_R, the perpendicular component $E_\perp$ decouples and the mixing is reduced to a 2D system given by the low-right sector in the second term of the left-side hand of Eq. (2). The term $\Delta_\parallel = \frac{1}{2}\omega(n_\parallel - 1)$ vanishes in the weak-dispersion limit, since the refraction index is $n_\parallel \sim 1$ for relativistic axions. The quantum-electrodynamics (QED) vacuum refraction parameter, Δ_Q, can be treated independently. We have defined the refraction parameter as $\Delta_p = -\omega_p^2/2\omega$ with $\omega_p = (e^2 n_e/m_e \varepsilon_0)^{1/2}$ being the characteristic frequency of the plasma, and the axion mass parameter is $\Delta_\phi = -m_\phi^2/2\omega$. The coupling term is $\Delta_M = g_{\phi\gamma} B/2$. We also define $\Delta k^2 = (\Delta_p + \Delta_Q - \Delta_\phi)^2 + 4\Delta_M^2$ and the mixing angle that holds the diagonalization, $\tan(2\theta_m) = 2\Delta_M/(\Delta_p - \Delta_\phi)$.

B. The role of the plasma density in the relative weight of QED corrections

It has been pointed out that the QED vacuum polarization effect acts as a suppressor of the axion-(keV)photon cross section in a minimal model of neutron star adopting

*javier.miguelhernandez@riken.jp

the Goldreich-Julian (GJ) corotation density, $n_{\rm GJ} = 4\pi\varepsilon_0 B(r)(eP)^{-1}$ [9,10]. However, a pair-multiplicity factor, defined as $\kappa = n_e/n_{\rm GJ}$, emerges in modern approaches beyond the GJ paradigm [11]. The ratio of plasma effects to QED vacuum effects, manifested through the Euler-Heisenberg term $\mathcal{L}_{\rm QED} = \frac{\alpha^2}{90m_e^4}[(F_{\mu\nu}F^{\mu\nu})^2 + \frac{7}{4}(F_{\mu\nu}\tilde{F}^{\mu\nu})^2]$, scales with the density profile across the gas [9,12]

$$\frac{\Delta_p}{\Delta_{Q_\perp}} = 5\times 10^{-10}\left(\frac{\rm keV}{\omega}\right)^2 \frac{10^8[\rm T]}{B(r)}\frac{1[\rm s]}{P}\kappa. \tag{3}$$

From Eq. (3) it follows that the tension with QED is progressively relaxed above $\kappa \gtrsim 10^5$ at relatively large distances from the star for keV photons, while Δ_Q gradually vanishes near its surface for $\kappa \gtrsim 10^8$. In the case of very energetic transitory events featured by magnetars, the charge density near the star surface is $n_e \sim 10^{30}$ cm^{-3} [13], many orders over the occupation number predicted by the GJ model. Although the density profile through the atmosphere of the 'fireball' is barely known, simulations suggest that pair-multiplicity factors $\kappa \lesssim 10^{10}$ are tenable at an altitude of a few stellar radii [14]. That renders resonant conversion efficient in the parameter space dominated by plasma effects, including highly-magnetic neutron stars, where $10^{4-5} \lesssim \kappa \lesssim 10^7$ [11,15], against previous expectations.

C. Magnetar axion

Magnetars are compact stellar remnants endowed with extreme magnetic fields, typically about 10^{10-11} T, with a 'canonical' mass around 10–20 solar masses and a rotation period of the order of seconds [16]. In the standard picture their persistent emission mechanisms involve pair-production and magnetic acceleration, catalyzing the migration of charges to higher altitudes from the star to give rise to curvature radiation, synchrotron emission, and inverse Compton scattering [17,18]. The beamed photons could be converted to axions through nonadiabatic resonant mechanism at their path across the nonrelativistic, 'cold' plasma of the magnetosphere [11,12,19–22]. In the aligned-rotator approximation, where the magnetic axis and the rotation axis, $\hat{z}$, are superimposed, the axion-photon oscillation amplitude is derived from introducing the resonance condition $\Delta_p - \Delta_\phi = 0$ in Eq. (2), yielding a conversion probability $\mathrm{P}_{\gamma\phi} = \Delta^2 \mathrm{k}/(2\frac{\partial}{\partial z}\Delta_p)$. Since outgoing photons present a gradient $\frac{\partial}{\partial z}\Delta_p \sim \mathrm{m}_\phi^2\omega^{-1}z_c^{-1}$, it is straightforward to obtain [11]

$$\mathrm{P}_{\gamma\phi} = \frac{\mathrm{g}_{\phi\gamma}^2 B^2(z_c)\omega z_c}{\mathrm{m}_\phi^2}. \tag{4}$$

In Eq. (4), $B(r) = B_0(\mathrm{R}/\mathrm{r})^3$ expresses the magnetic field in the dipole approximation, which is stationary as a result of an aligned rotator, as a function of the distance from the surface of the star; z_c is the conversion altitude, and ω the pulse of the photon.

III. MAGNETAR FLARES AND THEIR AXION COUNTERPART

A. Magnetar flares

The so-called anomalous x-ray pulsars (AXPs) and soft gamma-ray repeaters (SGRs) today are thought to be transient events from magnetars. Their strong outbursts are frequently referred to as short bursts (SBs), intermediate flares (IFs), and giant flares (GFs), whose more general characteristics are summarized in Table I. If the quiescent emission mechanisms of magnetars are poorly understood, the scenario for transient events is even more complex. Rapid magnetic field reconfiguration is thought to be an important part of the outbursts. The released magnetic energy is then converted to thermal energy in the magnetosphere—cf. [23] for solved nonthermal spectral features. However, the triggering mechanisms, and the exact role of the magnetic field remain unresolved. The timescale of the magnetic reconnection is $t_{\rm rec} \sim L/V$, where L is the height of the reconnection point and V is the inflow velocity. This should be much larger than the typical timescale of the system, $\tau_s \sim |\omega - \mathrm{m}_\phi|^{-1}$, to render the conversion mechanism described by Eq. (4) plausible. Within this scenario, reasonable for a relatively high frequency or a sufficiently high distance from the star, we have $\tau_s \ll t_{\rm rec}$ and the oscillation takes place in a pseudostationary regime. We include the spectra of an IF with energy scale about 10^{41} erg s^{-1} in Fig. 1 (left). The correlated axion flare is quantified in units of the typical occupation of virialized dark matter in the Galactic halo, around 10^{13} keV cm^{-2} s^{-1}.

We will confine our attention throughout the following sections to the study of axion giant flares (AGFs) triggered by GFs. Three 'Galactic' GFs have been observed; from SGR 0526-66, actually hosted by Large Magellanic Cloud (LMC), in 1979 [25], from SGR $1900+14$ in 1998 [26], and the most luminous to date, from SGR 1806–20 in 2004 [27,28]. Although there is consensus that GFs are rare events, the exact rate is a source of controversy and is susceptible to observational bias [29]. Statistics in [30] suggests that the rate for events above 4×10^{44} erg is $\sim 3.8\times 10^5$ Gpc^{-3} yr^{-1}, resulting in a event rate per

TABLE I. Properties of X/γ-ray emission from magnetars.

Feature	Object	Timescale[a] (s)	L[b] (erg s^{-1})
Quiescent	Magnetar	…	10^{33}[c]
SB	AXP and SGR	0.2–1	10^{39-41}
IF	AXP and SGR	1–40	10^{41-43}
GF	SGR	$<0.5+$ tail[d]	10^{44-47}

[a]Duration of the peak.
[b]Bolometric luminosity; isotropic flux.
[c]Typical value with a variability of several orders of magnitude.
[d]A few hundred seconds scattering tail with a lower luminosity follows the main peak.

magnetar of the order of $\lesssim 0.02\ \mathrm{yr}^{-1}$. These estimates rely on the strong evidence that 1–20% of the gamma ray burst (GRB) sample are indeed extragalactic GFs, whose tails are undetectable due to the large distance [13].

In that manner, the catalog of confirmed GFs is poor and, in addition, their spectral features are not adequately characterized due to saturation of the detectors and other systematics. Therefore, we fit and extend to low frequency a black-body (BB) curve at a temperature $k_B T_{\mathrm{BB}} \sim 175$ keV, with a fluence of $1.36\ \mathrm{erg\,cm}^{-2}$ of >30 keV photons on Earth consistent with the SGR 1806–20 event [27], to be employed in simulations throughout the following sections. Notwithstanding that empirical data are not available when referring to the polarization of the GF, it is predicted that the strong magnetic field in magnetars linearly polarizes the photons in two normal modes, i.e., ordinary (O), with the E field lying on the k-B plane, and extraordinary (X). The weight of the O-mode, which efficiently mixes with axion, was established in a conservative 0.5 fraction for our estimates after consulting the literature [31–34].

B. The flight of axion to Earth

Obviously, both the photon and axion flux suffer from the inverse-square law with distance. Moreover, axions with a rest mass $\lesssim 10^{-5}$ eV crossing through several cosmic magnetic domains, with a typical length scale, s, of the order of Mpc, are reconverted efficiently into photons; first across their outgoing path through the intergalactic medium (IGM), and then upon reaching the Milky Way (MW) [35–37]. The photon-to-axion conversion probability derived from Eq. (2) is read $\mathrm{P}_{\gamma\phi} = 4\Delta_{\mathrm{M}}^2 \sin^2(\ell \Delta \mathrm{k}/2)/\Delta^2 \mathrm{k}$. In the strong-coupling limit, the inequality $(\Delta_p + \Delta_Q - \Delta_\phi)^2 \ll 4\Delta_{\mathrm{M}}^2$ is obtained, resulting in the well-known expression [38]

$$\mathrm{P}_{\phi\gamma} = \frac{\mathrm{g}_{\phi\gamma}^2 B^2 \ell^2}{4}. \tag{5}$$

From a panoramic perspective, our galaxy takes the form of a thin disk of ~30 kpc length, i.e., $\ell \ll s$, with a magnetic field of the order of a fraction of nT, and a low-electron density, about $10^{-3}\ \mathrm{cm}^{-3}$. Crucially, from Eq. (5) it follows that only a marginal fraction of the magnetar axions released in the vicinity of the MW are reconverted into photons during their approximation to Earth. In other words, the astroparticle flux density at origin, determined by Eq. (4), approximately persists.

Photons are massless through the IGM. The axion is massive. In contrast to the plasma that envelopes the magnetosphere, where the resonant conversion takes place at $\omega_p \sim \mathrm{m}_\phi$, the relation $\hbar\omega \sim \gamma \mathrm{m}_\phi$ is maintained through the vacuum, with γ being the Lorentz factor. The axion velocity is $\beta_\phi = \sqrt{1 - 1/\gamma^2}$. In that form, the delay time at keV energies for values of the Lorentz factor between 10^{1-7} and pair-multiplicity factor $10^2 \lesssim \kappa \lesssim 10^9$ varies between about a year per traveled kpc and a few milliseconds. That would render photon-axion multimessenger astronomy constrained to a human-scale time frame and would motivate the tracking of confirmed outbursts for relatively massive axions.

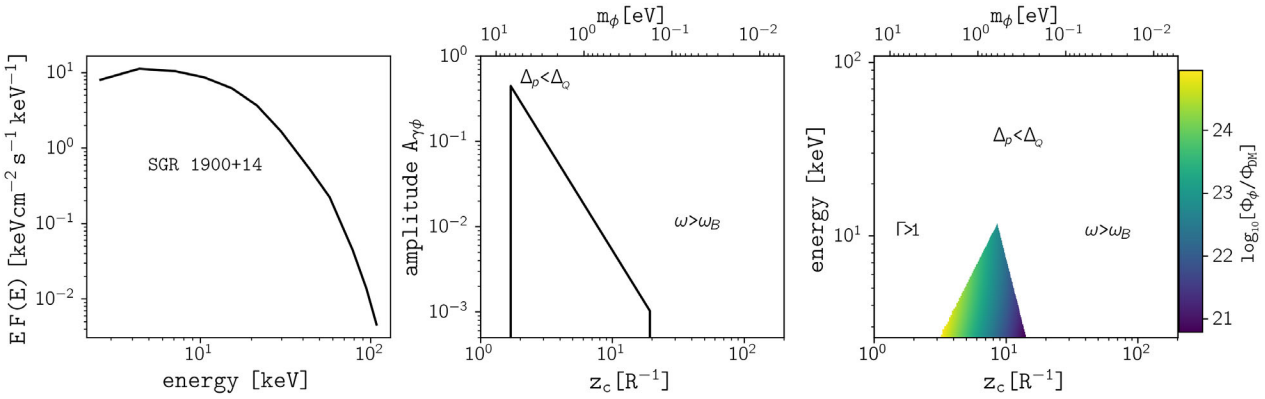

FIG. 1. Left: Deconvolved spectra of an intermediate flare (IF) from SGR 1900 + 14 occurred on 2001 July 2 with a duration of several seconds. It combines FREGATE data between 7–150 keV and WXM data between 2–25 keV. The bolometric luminosity was $\gtrsim 10^{41}\ \mathrm{erg\,s}^{-1}$. We consider and therefore represent a 50% fraction of the incoming beam polarized in the O-mode. Adapted from [24]. Middle: Photon-to-axion oscillation amplitude at ~keV energy as a function of the resonance altitude, $\mathrm{z_c}$, in units of the stellar radius or axion mass, m_ϕ. Right: Axion flux density, Φ_ϕ, triggered by the IF in units of ambient dark matter (DM) density, Φ_{DM}, over altitude or axion mass. The pair-multiplicity factor over the Goldreich-Julian corotation density is defined $\kappa = n_e/n_{\mathrm{GJ}}$ and set $\kappa \sim 10^8$. The rotation period $P \sim 1$ s, $B_0 \sim 10^{10}$, T and R $\sim 10^6$ cm are canonical dimensions. We adopt QCD axion-coupling strength. The nonadiabatic resonant model is ruled out in sectors where O-modes become evanescent, or equivalently $\omega_p > \omega$; $\Gamma \gtrsim 1$ regions, being Γ the adiabaticity factor of the system; 'weak-field' zones, with $\omega \gtrsim \omega_B$ being $\omega_B = eB(z_c)/m_e$ the gyrofrequency; sectors where the QED vacuum polarization effect governs the dispersion relations, or $\Delta_p < \Delta_Q$. As a consequence, axions with $\mathrm{m}_\phi \gtrsim 10^{-1}$ eV mix efficiently with 1–10 keV photons.

IV. OBSERVABLE EFFECTS

A. Detection of axion flares through inverse Primakoff-effect

The solar axion spectrum is formed by interactions of axion with SM particles in the internal plasma of the star. A spectrum dominated by Primakoff-effect presents a maximal flux about 10^9 cm^{-2} s^{-1} at 3–4 keV for an axion-photon coupling strength $g_{\phi\gamma} \sim 10^{-11}$ GeV^{-1}. A solar spectrum shaped by atomic recombination and deexcitation, bremsstrahlung, and Compton (ABC) processes peaks a similar fluence around 1 keV for an axion-electron coupling constant $g_{\phi e} \sim 10^{-13}$. Differently from magnetar axion, where one finds from Eq. (4) that the QCD axion flux is enhanced for x-ray photons, the emitted solar flux scales with g^2 mitigating the emission of axionlike particles (ALPs) with a low coupling strength, including both KSVZ [39,40] and DFSZ [41,42] axions.

Helioscopes are directional detectors tracking the Sun [43–46]. Their working principle relies on inverse Primakoff axion-to-photon conversion, $\phi + \gamma_{\rm virt} \to \gamma$, in a magnetized cryostat equipped with photomultiplier tubes (PMTs). The cross section of helioscopes in the limit $q\ell \ll 1$ is given by Eq. (5), with q being the transfer of momenta between the axion and the photon and ℓ being the length of flight across the vessel. The product of the density of the magnetic field and the length/area is restricted in a physical implementation. On the other hand, coherence is gradually lost for $m_\phi \gtrsim 10^{-2}$ eV. The sensitivity of helioscopes in terms of the axion-photon coupling strength is approximately [47]

$$g_{\phi\gamma}[\mathrm{GeV}^{-1}] \gtrsim 1.4 \times 10^{-9} \frac{b^{1/8}}{t^{1/8}(B\ell[\mathrm{T}\cdot\mathrm{m}])^{1/2}(\mathrm{A}[\mathrm{cm}^2])^{1/4}} \times \left(\frac{\Phi_\phi}{\Phi_\odot}\right)^{-1/2}, \tag{6}$$

where b is the integrated background noise in the energy range 1–10 keV, t is exposure time, A is the transverse area of the detector, and Φ_ϕ is the received flux in units of $\Phi_\odot$ which is the integrated flux of solar axions on Earth.

Helioscope-type apparatus can be employed to search for axion flares. In Fig. 2 we qualitatively compare solar and magnetar scanning performed by an IAXO-like instrument [48,54]. There, we find a volume of special interest in a $\lesssim$3 kpc radius from Earth, with around three dozen cataloged magnetars, with about 1/3 of them being within a 1/2 kpc radius, while the closest object is at a distance of about 0.1 kpc [49].

B. Observation of axion flares using liquid-xenon detectors

Experiments storing liquid xenon are sensitive to axion through the axioelectric effect, $\phi + e + Z \to e' + Z$, sustained by Eq. (1). In the relativistic limit, the cross section reads

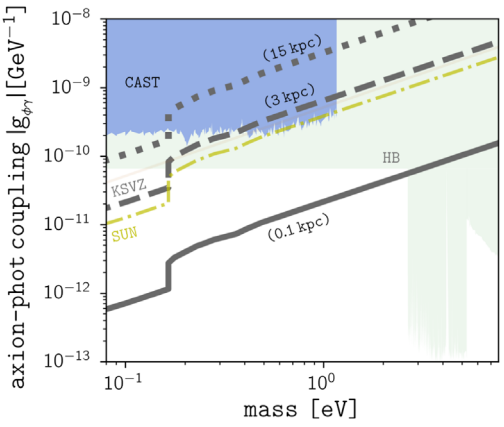

FIG. 2. Limit on the sensitivity to axion flares by realistic helioscope-like detectors, based on the inverse Primakoff effect. The CAST helioscope limit is established at 95% confidence level (CL) [50]. The horizontal-branch (HB) exclusion region is established by indirect methods at 95% CL [51]. Astrobounds established by indirect methods are also included in green [52,53]. The light brown solid line represents the KSVZ axion. The dot-dash yellow line projects new-generation helioscope sensitivity at 95% CL from a campaign lasting several years [54], while the duration of the giant flare is set $t = 0.125$ s. Dark lines correspond to direct detection of GFs with 15 (dotted), 3 (dashed), and 0.1 (solid) kpc distance, at 95% CL. The comparison is performed by integration of the spectral functions between 1–10 keV, where the detectors are more sensitive coinciding with the maximal flux of solar axion.

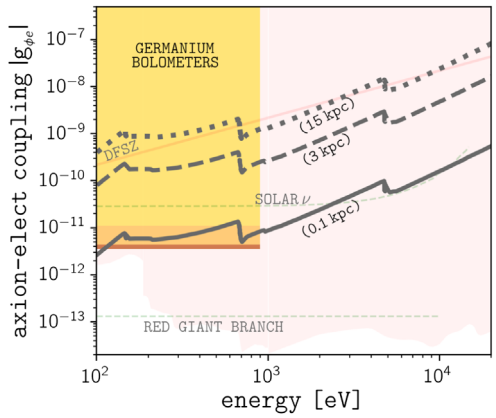

FIG. 3. Limit on the sensitivity to AGFs based on the axioelectric effect for realistic liquid xenon detectors. The regions shaded in warm colors are established by direct detection of solar axion at 90% CL [58–60]. Dashed light-green lines project stellar hints [61–63]. The light reddish zone corresponds to methods whose hypothesize that all the dark matter in the halo is formed of axion and a high homogeneity, overlapping other model-dependent, or indirect, results [58–60,64,65]. Dark lines correspond with direct detection of giant flares with 15 (dotted), 3 (dashed), and 0.1 (solid) kpc distance, at 95% CL. The red solid line corresponds with DFSZ, nonrelativistic axion. Parameters are $t = 0.125$ s, $\mathrm{W} = 10^4$ kg, $\mathfrak{R} = 0.3137\sqrt{\mathrm{keV}}$, $b = 1.4 \times 10^{-5}$, and s^{-1} kg^{-1} keV^{-1}.

$$\sigma_{\phi e}[\mathrm{cm}^2\,\mathrm{kg}^{-1}] \simeq 10^2 \times g_{\phi e}^2 \left(\frac{\mathrm{E}}{\mathrm{keV}}\right)^2 \times \left(\frac{\sigma_{pe}(\mathrm{E})}{10^6\,\mathrm{b\,atom}^{-1}}\right), \quad (7)$$

where the proton-electron cross section σ_{pe} (E) can be, e.g., interpolated from [55]. By the introduction of an expectation signal-to-noise ratio (SNR) in Eq. (7) it is possible to write the sensitivity of liquid-xenon detectors in terms of the axion-electron coupling strength [56]

$$g_{\phi e} \gtrsim 10^{-1} \left(\frac{\mathrm{keV}}{\mathrm{E}}\right) \times \left(\frac{10^6\,\mathrm{b\,atom}^{-1}}{\sigma_{pe}(\mathrm{E})}\right)^{1/2} \times \sqrt{\mathrm{SNR}} \left(\frac{4\mathfrak{R} b\sqrt{\mathrm{E}}}{t \times \mathrm{W}}\right)^{1/4} \times \Phi_\phi^{-1/2}, \quad (8)$$

where $\mathfrak{R}$ is the spectral resolution of the instrument, b is the background event rate, t is integration time, and W is weight of the stored xenon. In Fig. 3 we represent the sensitivity to AGFs for XAX-like experiments [57].

V. CONCLUSIONS

The conversion of the beam of light emitted from highly-magnetic neutron stars into relativistic axions, first at their magnetospheres and then during their flight to Earth, opens a new window for the direct detection of axions or for revisiting and extending exclusion limits which arbitrarily assume that axionlike particles form all the dark matter in the nearby universe, and that the DM is distributed homogeneously. In this paper we pioneered the concept of photon-axion multimessenger astronomy with giant flares, a type of rare event featured by soft gamma-ray repeaters that can be, for a fraction of a second, more luminous than hundred times the brightest supernovae [66,67], or almost 10^{14} suns radiating coherently, with an uncertain upper bound, as more magnetic magnetars could release GFs 1–2 orders brighter than the strongest event observed to date if we only take into account stored magnetic energy [27].

Giant flares could correlate with an axion counterpart via resonant mixing through the magnetosphere. Anticipating a short term at which the SGR catalog is more extensive and their characteristics better understood, we analyze sensitivities to axion bursts in the soft x-ray energy range for realistic experiments. Under a number of idealizations of recurring use in related works, we find that GFs originating in the vicinity of Earth would provide the detectors with sensitivity to axionlike particles with an axion-photon coupling $g_{\phi\gamma} \gtrsim$ several $\times\, 10^{-13}$ GeV^{-1} and axion-electron coupling $g_{\phi e} \gtrsim$ few $\times\, 10^{-12}$ at 95% CL over a broad range and for reasonable benchmark parameters. A confirmed detection would result in an absolute "spectrum," while for the projection of new exclusion bounds the sensitivity would be calibrated against data from x-ray telescopes and grounded by theory. The expected axion-flux density on Earth results from the convolution of three terms; the GF photon spectral flux density, the photon-to-axion conversion probability, and the geometric dilution with distance. As a reference, for an upper-limit photon-axion conversion probability $\mathcal{O}(1/2)$, the flare from SGR 1806–20—10^{46} erg, 15 kpc distance—would result in a transient influence on Earth similar to the flux of solar axions for an axion-photon coupling strength $g_{\phi\gamma} \sim 10^{-11}$ GeV^{-1}.

Assuming axion, this work predicts the existence of AGFs across our Universe, and perhaps their detectability by ground-based observatories. Transcendentally, the echo of a galactic flare might be received today in the form of AGF, due to the delay time that massive particles suffer compared to ordinary photons during their flight through the interstellar medium. Thus, monitoring the confirmed sources of giant flares—SGR 0526-66, 48 kpc distant, in 1979; SGR 1900 + 14, 6 kpc distant, in 1998; and SGR 1806-20 in 2004—with dark matter detectors, in addition to future events, can be motivated—e.g., during hours when helioscopes cannot track the Sun. A state-of-the-art estimate of the event rate suggests that each magnetar releases up to one potent giant flare every fifty years [30]. There are currently more than four dozen cataloged magnetars within a radius of 15 kpc from Earth. Therefore, the probability of an observable AGF event would be in the order of a dozen in the next decade, with approximately 2/3 of them originating within a distance of 3 kpc. In addition, it is striking that, although the bursts themselves are not periodic, the activity might only occur during predictable periodic intervals [68]. As a consequence, the prediction and tracking of magnetars entering an active period using dedicated axiotelescopes, or a network, is not discardable in order to enhance the probability of detection through the observation of stars with active, nonoverlapping windows.

Finally, the XENON1T Collaboration recently reported an electronic recoil excess below 7 keV compatible with solar axion at 3.4σ CL [69]. However, the precise parameter space is in tension with stellar evolution at 8σ [70]. Interestingly, magnetar axions could mimic solar axion at keV energies without conflicting with stellar physics. However, the signal persisted for a large time interval incompatible with the known nature of magnetar flares, while quiescent isolated sources would be too distant to provide the deposited energy. Magnetar axion count rate could be a factor to consider in future experiments.

ACKNOWLEDGMENTS

This work was supported by the Special Postdoctoral Researchers (SPDR) program. J. D. M. appreciates having been invited as a visiting researcher of the Instituto de Astrofísica de Canarias (IAC) for a period coinciding with a part of this research.

[1] S. Weinberg, A new light boson?, Phys. Rev. Lett. **40**, 223 (1978).
[2] F. Wilczek, Problem of Strong p and t Invariance in the Presence of Instantons, Phys. Rev. Lett. **40**, 279 (1978).
[3] R. D. Peccei and H. R. Quinn, CP Conservation in the Presence of Pseudoparticles, Phys. Rev. Lett. **38**, 1440 (1977).
[4] L. Abbott and P. Sikivie, A cosmological bound on the invisible axion, Phys. Lett. **120B**, 133 (1983).
[5] M. Dine and W. Fischler, The not-so-harmless axion, Phys. Lett. **120B**, 137 (1983).
[6] J. Preskill, M. B. Wise, and F. Wilczek, Cosmology of the invisible axion, Phys. Lett. **120B**, 127 (1983).
[7] Particle Data Group, Review of particle physics, Phys. Rev. D **98**, 030001 (2018).
[8] F. Wilczek, Two Applications of Axion Electrodynamics, Phys. Rev. Lett. **58**, 1799 (1987).
[9] G. Raffelt and L. Stodolsky, Mixing of the photon with low-mass particles, Phys. Rev. D **37**, 1237 (1988).
[10] P. Goldreich and W. H. Julian, Pulsar electrodynamics, Astrophys. J. **157**, 869 (1969).
[11] J. De Miguel and C. Otani, Superdense beaming of axion dark matter in the vicinity of the light cylinder of pulsars, arXiv:2111.01746.
[12] F. P. Huang, K. Kadota, T. Sekiguchi, and H. Tashiro, Radio telescope search for the resonant conversion of cold dark matter axions from the magnetized astrophysical sources, Phys. Rev. D **97**, 123001 (2018).
[13] O. J. Roberts *et al.*, Rapid spectral variability of a giant flare from a magnetar in NGC 253, Nature (London) **589**, 207 (2021).
[14] Y.-P. Yang and B. Zhang, On the polarization properties of magnetar giant flare pulsating tails, Astrophys. J. **815**, 45 (2015).
[15] C. Guépin, B. Cerutti, and K. Kotera, Proton acceleration in pulsar magnetospheres, Astron. Astrophys. **635**, A138 (2020).
[16] R. C. Duncan and C. Thompson, Formation of very strongly magnetized neutron stars—implications for gamma-ray bursts, Astrophys. J. **392** (1992).
[17] M. A. Ruderman and P. G. Sutherland, Theory of pulsars: Polar gaps, sparks, and coherent microwave radiation, Astrophys. J. **196**, 51 (1975).
[18] J. Arons and E. T. Scharlemann, Pair formation above pulsar polar caps: Structure of the low altitude acceleration zone., Astrophys. J. **231**, 854 (1979).
[19] D. Lai and J. Heyl, Probing axions with radiation from magnetic stars, Phys. Rev. D **74**, 123003 (2006).
[20] R. Perna, W. C. G. Ho, L. Verde, M. van Adelsberg, and R. Jimenez, Signatures of photon-axion conversion in the thermal spectra and polarization of neutron stars, Astrophys. J. **748**, 116 (2012).
[21] R. A. Battye, B. Garbrecht, J. I. McDonald, F. Pace, and S. Srinivasan, Dark matter axion detection in the radio/mm waveband, Phys. Rev. D **102**, 023504 (2020).
[22] A. Zhuravlev, S. Popov, and M. Pshirkov, Photon-axion mixing in thermal emission of isolated neutron stars, Phys. Lett. B **821**, 136615 (2021).
[23] S. E. Boggs, A. Zoglauer, E. Bellm, K. Hurley, R. P. Lin, D. M. Smith, and C. Wigger, The giant flare of December 27, 2004 from SGR 1806-20, Astrophys. J. **661**, 458 (2007).
[24] J. F. Olive, K. Hurley, T. Sakamoto, J. L. Atteia, G. Crew, G. Ricker, G. Pizzichini, C. Barraud, and N. Kawai, Time-resolved x-ray spectral modeling of an intermediate burst from SGR 1900 + 14 observed by HETE-2 FREGATE and WXM, Astrophys. J. **616**, 1148 (2004).
[25] E. P. Mazets, S. Golenetskii, V. N. Il'inskii, R. L. Aptekar, and Y. A. Guryan, Observations of a flaring x-ray pulsar in dorado, Nature (London) **282**, 587 (1979).
[26] K. Hurley *et al.*, A Giant, periodic flare from the soft gamma repeater SGR1900 + 14, Nature (London) **397**, 41 (1999).
[27] K. Hurley, S. E. Boggs, D. M. Smith, R. C. Duncan, R. Lin, A. Zoglauer, S. Krucker, G. Hurford, H. Hudson, C. Wigger, W. Hajdas, C. Thompson, I. Mitrofanov, A. Sanin, W. Boynton, C. Fellows, A. von Kienlin, G. Lichti, A. Rau, and T. Cline, An exceptionally bright flare from SGR 1806-20 and the origins of short-duration γ-ray bursts, Nature (London) **434**, 1098 (2005).
[28] D. M. Palmer *et al.*, A giant γ-ray flare from the magnetar SGR 1806–20, Nature (London) **434**, 1107 (2005).
[29] K. Hurley, The short gamma-ray burst—sgr giant flare connection, Adv. Space Res. **47**, 1337 (2011).
[30] E. Burns *et al.*, Identification of a local sample of gamma-ray bursts consistent with a magnetar giant flare origin, Astrophys. J. Lett. **907**, L28 (2021).
[31] Y. E. Lyubarsky, On the x-ray spectra of soft gamma repeaters, Mon. Not. R. Astron. Soc. **332**, 199 (2002).
[32] Y.-P. Yang and B. Zhang, On the polarization properties of magnetar giant flare pulsating tails, Astrophys. J. **815**, 45 (2015).
[33] T. van Putten, A. L. Watts, M. G. Baring, and R. A. M. J. Wijers, Radiative transfer simulations of magnetar flare beaming, Mon. Not. R. Astron. Soc. **461**, 877 (2016).
[34] R. Taverna and R. Turolla, On the spectrum and polarization of magnetar flare emission, Mon. Not. R. Astron. Soc. **469**, 3610 (2017).
[35] S. V. Krasnikov, New Astrophysical Constraints on the Light-Pseudoscalar–Photon Coupling, Phys. Rev. Lett. **76**, 2633 (1996).
[36] M. Simet, D. Hooper, and P. D. Serpico, Milky Way as a kiloparsec-scale axionscope, Phys. Rev. D **77**, 063001 (2008).
[37] M. Fairbairn, T. Rashba, and S. Troitsky, Photon-axion mixing and ultra-high energy cosmic rays from BL Lac type objects: Shining light through the Universe, Phys. Rev. D **84**, 125019 (2011).
[38] K. van Bibber, P. M. McIntyre, D. E. Morris, and G. G. Raffelt, Design for a practical laboratory detector for solar axions, Phys. Rev. D **39**, 2089 (1989).
[39] J. E. Kim, Weak-Interaction Singlet and Strong CP Invariance, Phys. Rev. Lett. **43**, 103 (1979).
[40] M. A. Shifman, A. Vainshtein, and V. I. Zakharov, Can confinement ensure natural cp invariance of strong interactions, Nucl. Phys. **166**, 493 (1980).
[41] M. Dine, W. Fischler, and M. Srednicki, A simple solution to the strong cp problem with a harmless axion, Phys. Lett. **104B**, 199 (1981).

[42] A. P. Zhitnitskii, Possible suppression of axion-hadron interactions, Sov. J. Nucl. Phys. **31** (1980).
[43] P. Sikivie, Experimental Tests of the "Invisible" Axion, Phys. Rev. Lett. **51**, 1415 (1983).
[44] D. M. Lazarus, G. C. Smith, R. Cameron, A. C. Melissinos, G. Ruoso, Y. K. Semertzidis, and F. A. Nezrick, Search for Solar Axions, Phys. Rev. Lett. **69**, 2333 (1992).
[45] S. Moriyama, M. Minowa, T. Namba, Y. Inoue, Y. Takasu, and A. Yamamoto, Direct search for solar axions by using strong magnetic field and x-ray detectors, Phys. Lett. B **434**, 147 (1998).
[46] K. Zioutas *et al.* (CAST Collaboration), First Results from the Cern Axion Solar Telescope, Phys. Rev. Lett. **94**, 121301 (2005).
[47] J. I. Collar *et al.* (CAST Collaboration), CAST: A search for solar axions at CERN, in *Conference on Astronomical Telescopes and Instrumenation* (2003), arXiv:hep-ex/0304024.
[48] E. Armengaud *et al.* (IAXO Collaboration), Physics potential of the international axion observatory (IAXO), J. Cosmol. Astropart. Phys. 06 (2019) 047.
[49] F. Coti Zelati, N. Rea, J. A. Pons, S. Campana, and P. Esposito, Systematic study of magnetar outbursts, Mon. Not. R. Astron. Soc. **474**, 961 (2018).
[50] V. Anastassopoulos *et al.* (CAST Collaboration), New CAST limit on the axion-photon interaction, Nat. Phys. **13**, 584 (2017).
[51] A. Ayala, I. Domínguez, M. Giannotti, A. Mirizzi, and O. Straniero, Revisiting the Bound on Axion-Photon Coupling from Globular Clusters, Phys. Rev. Lett. **113**, 191302 (2014).
[52] M. Regis, M. Taoso, D. Vaz, J. Brinchmann, S. L. Zoutendijk, N. F. Bouché, and M. Steinmetz, Searching for light in the darkness: Bounds on ALP dark matter with the optical MUSE-faint survey, Phys. Lett. B **814**, 136075 (2021).
[53] D. Grin, G. Covone, J.-P. Kneib, M. Kamionkowski, A. Blain, and E. Jullo, A telescope search for decaying relic axions, Phys. Rev. D **75**, 105018 (2007).
[54] I. G. Irastorza *et al.*, Towards a new generation axion helioscope, J. Cosmol. Astropart. Phys. 06 (2011) 013.
[55] W. Veigele, Photon cross sections from 0.1 kev to 1 mev for elements $z = 1$ to $z = 94$, At. Data Nucl. Data Tables **5**, 51 (1973).
[56] K. Arisaka, P. Beltrame, C. Ghag, J. Kaidi, K. Lung, A. Lyashenko, R. D. Peccei, P. Smith, and K. Ye, Expected sensitivity to galactic/solar axions and bosonic super-WIMPs based on the axio-electric effect in liquid XENON dark matter detectors, Astropart. Phys. **44**, 59 (2013).
[57] K. Arisaka, H. Wang, P. Smith, D. Cline, A. Teymourian, E. Brown, W. Ooi, D. Aharoni, C. Lam, K. Lung, S. Davies, and M. Price, XAX: A multi-ton, multi-target detection system for dark matter, double beta decay and pp solar neutrinos, Astropart. Phys. **31**, 63 (2009).
[58] E. Armengaud *et al.* (EDELWEISS Collaboration), Searches for electron interactions induced by new physics in the EDELWEISS-III Germanium bolometers, Phys. Rev. D **98**, 082004 (2018).
[59] D. S. Akerib *et al.* (LUX Collaboration), First Searches for Axions and Axionlike Particles with the LUX Experiment, Phys. Rev. Lett. **118**, 261301 (2017).
[60] C. Fu *et al.* (PandaX Collaboration), Limits on Axion Couplings from the First 80 Days of Data of the PandaX-II Experiment, Phys. Rev. Lett. **119**, 181806 (2017).
[61] P. Gondolo and G. G. Raffelt, Solar neutrino limit on axions and keV-mass bosons, Phys. Rev. D **79**, 107301 (2009).
[62] F. Capozzi and G. Raffelt, Axion and neutrino bounds improved with new calibrations of the tip of the red-giant branch using geometric distance determinations, Phys. Rev. D **102**, 083007 (2020).
[63] O. Straniero, C. Pallanca, E. Dalessandro, I. Dominguez, F. R. Ferraro, M. Giannotti, A. Mirizzi, and L. Piersanti, The RGB tip of galactic globular clusters and the revision of the axion-electron coupling bound, Astron. Astrophys. **644**, A166 (2020).
[64] C. O'Hare, cajohare/axionlimits: Axionlimits (2020).
[65] L. D. Luzio, M. Fedele, M. Giannotti, F. Mescia, and E. Nardi, Stellar evolution confronts axion models, J. Cosmol. Astropart. Phys. 02 (2022) 035.
[66] S. Dong *et al.*, ASASSN-15lh: A highly super-luminous supernova, Science **351**, 257 (2016).
[67] E. Kankare *et al.*, A population of highly energetic transient events in the centres of active galaxies, Nat. Astron. **1**, 865 (2017).
[68] M. Denissenya, B. Grossan, and E. V. Linder, Distinguishing time clustering of astrophysical bursts, Phys. Rev. D **104**, 023007 (2021).
[69] E. Aprile *et al.* (XENON Collaboration), Excess electronic recoil events in XENON1T, Phys. Rev. D **102**, 072004 (2020).
[70] L. Di Luzio, M. Fedele, M. Giannotti, F. Mescia, and E. Nardi, Solar Axions Cannot Explain the XENON1T Excess, Phys. Rev. Lett. **125**, 131804 (2020).